




Article

Engineering the Activity of Old Yellow Enzyme NemR-PS for Efficient Reduction of (*E/Z*)-Citral to (*S*)-Citronellol

Binbin Feng¹, Xia Li¹, Lijun Jin¹, Yi Wang¹, Yi Tang¹, Yuhao Hua¹, Chenze Lu² , Jie Sun¹, Yinjun Zhang^{1,*} 
and Xiangxian Ying^{1,3,*} 

¹ Key Laboratory of Bioorganic Synthesis of Zhejiang Province, College of Biotechnology and Bioengineering, Zhejiang University of Technology, Hangzhou 310014, China; fengbinbin1997@163.com (B.F.); lixia970419@163.com (X.L.); jinlijun130@163.com (L.J.); huzai ziy@163.com (Y.W.); ty12150102@163.com (Y.T.); hyhua0616@163.com (Y.H.); jsun@zjut.edu.cn (J.S.)

² College of Life Sciences, China Jiliang University, Hangzhou 310018, China; chenzelu@cjlu.edu.cn

³ Zhejiang Invertin Biotechnology Co., Ltd., Huzhou 313000, China

* Correspondence: zhangyj@zjut.edu.cn (Y.Z.); yingxx@zjut.edu.cn (X.Y.)

Abstract: The cascade catalysis of old yellow enzyme, alcohol dehydrogenase and glucose dehydrogenase has become a promising approach for one pot, two-step reduction of (*E/Z*)-citral to (*S*)-citronellol, serving as a chiral alcohol with rose fragrance. During the multi-enzymatic cascade catalysis, old yellow enzyme is responsible for the reduction of the conjugated C=C and the introduction of the chiral center, requiring high activity and (*S*)-enantioselectivity. Herein, to improve the activity of the old yellow enzyme from *Providencia stuartii* (NemR-PS) with strict (*S*)-enantioselectivity, the semi-rational design on its substrate binding pocket was performed through a combination of homology modeling, molecular docking analysis, alanine scanning and iterative saturation mutagenesis. The NemR-PS variant D275G/F351A with improved activity was obtained and then purified for characterization, obeying the substrate inhibition kinetics. Compared with the wild type, the parameters K_i and K_{cat}/K_m were increased from 39.79 mM and $2.09\text{ s}^{-1}\text{mM}^{-1}$ to 128.50 mM and $5.01\text{ s}^{-1}\text{mM}^{-1}$, respectively. Moreover, the variant D275G/F351A maintained strict (*S*)-enantioselectivity, avoiding the trade-off effect between activity and enantioselectivity. Either the enzyme NemR-PS or the variant D275G/F351A was co-expressed with alcohol dehydrogenase from *Yokenella* sp. WZY002 (YsADH) and glucose dehydrogenase from *Bacillus megaterium* (BmGDH_{M6}). In contrast to the whole-cell biocatalyst co-expressing NemR-PS, that co-expressing the variant D275G/F351A shortened the reaction time from 36 h to 12 h in the reduction of 400 mM (*E/Z*)-citral. In the manner of substrate constant feeding, the accumulated product concentration reached up to 500 mM and completely eliminate the residual intermediate and by-product, suggesting the effectiveness of protein engineering and substrate engineering to improve catalytic efficiency.

Keywords: (*S*)-citronellol; old yellow enzyme; semi-rational design; cascade catalysis; substrate feeding



Citation: Feng, B.; Li, X.; Jin, L.; Wang, Y.; Tang, Y.; Hua, Y.; Lu, C.; Sun, J.; Zhang, Y.; Ying, X. Engineering the Activity of Old Yellow Enzyme NemR-PS for Efficient Reduction of (*E/Z*)-Citral to (*S*)-Citronellol. *Catalysts* **2022**, *12*, 631. <https://doi.org/10.3390/catal12060631>

Academic Editors: Melinda Fogarasi, Anca Farcas and Oana Lelia Pop

Received: 11 May 2022

Accepted: 7 June 2022

Published: 9 June 2022

Publisher's Note: MDPI stays neutral with regard to jurisdictional claims in published maps and institutional affiliations.



Copyright: © 2022 by the authors. Licensee MDPI, Basel, Switzerland. This article is an open access article distributed under the terms and conditions of the Creative Commons Attribution (CC BY) license (<https://creativecommons.org/licenses/by/4.0/>).

1. Introduction

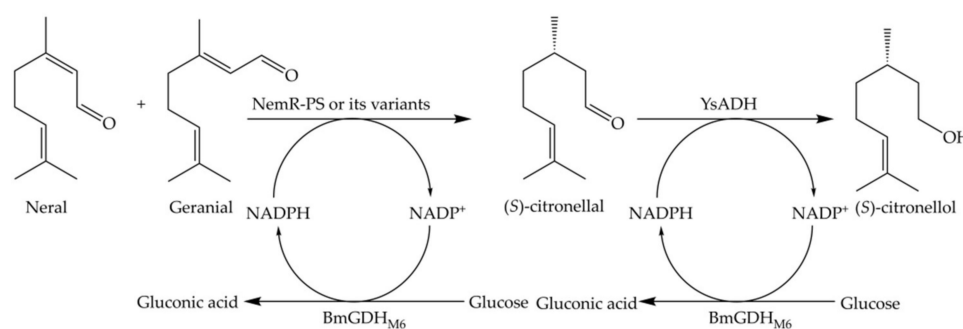
(*S*)-Citronellol is a chiral monoterpene alcohol which has more elegant aroma than its (*R*)-enantiomer [1,2]. As a raw material, (*S*)-citronellol can be used for stereoselective synthesis of (-)-*cis*-rose oxide [3]. The synthesis of citronellol often relies on the chemical methods using citral, geraniol or citronellal as starting raw material [4,5]. Chemical processes usually have poor regio- and enantio-selectivity and thus cannot meet the need of the synthesis of (*S*)-citronellol [6]. Meanwhile, enzymatic catalysis with superior selectivity is considered as a promising alternative of organic synthesis [7]. In a lately developed enzymatic process, (*S*)-citronellol was synthesized from one-pot, two-step reduction of (*E/Z*)-citral through the cascade catalysis of old yellow enzyme, alcohol dehydrogenase and glucose dehydrogenase. Specifically, *N*-ethylmaleimide reductase from *Providencia stuartii*

(NemR-PS, a member of the old yellow enzyme family) with strict (*S*)-enantioselectivity catalyzed the reduction of (*E/Z*)-citral to (*S*)-citronellal and alcohol dehydrogenase from *Yokenella* sp. WZY002 (YsADH) further reduced (*S*)-citronellal to (*S*)-citronellol, meanwhile glucose dehydrogenase from *Bacillus megaterium* (BmGDH_{M6}) together with glucose was responsible for coenzyme regeneration [7,8]. Among the enzymes, the specific activity of old yellow enzyme NemR-PS was relatively low and its activity improvement was needed for commercial use of the process [9].

Protein engineering proves to be effective for activity improvement and successful examples engineering old yellow enzyme are accumulating [10]. Through iterative saturation mutagenesis, directed evolution of the old yellow enzyme YqjM resulted in the most active variant Cys26Asp/Ile69Thr with 130-fold rate improvement in the reduction of 3-methylcyclohexenone [11]. Relying on GC analysis, screening workload could be formidable in the directed evolution of old yellow enzyme, whereas the structure-guided rational design offers smaller and smarter mutant library. A structure-guided engineering strategy focusing on the active sites was applied to the old yellow enzyme OYE2p, generating highly active variant Y84V with a 71.3% increase in catalytic efficiency towards (*E*)-citral [12]. Notably, the stereoselectivity of Y84V was improved from 89.2% to 98.0% in the reduction in (*E/Z*)-citral, avoiding the frequently-encountered trade-off effect between activity and enantioselectivity.

During multi-enzymatic cascade catalysis, improving catalytic efficiency of the process requires not only the engineering of a key enzyme but also biocatalyst and process engineering. In contrast to free enzymatic catalysis, the use of whole-cell biocatalyst co-expressing the enzymes protects the structural stability of the enzymes and improve the efficiency of mass transfer between enzymes [13,14]. During whole-cell biocatalyst, the expression level of multiple participating enzymes may differ, each enzymatic reaction often does not reach the optimal conditions. Thus, the accumulation of intermediates and by-products is often encountered. Careful investigation of the parameter affecting the process would facilitate to improve the catalytic efficiency and eliminate the residual intermediate and by-product [14,15].

Herein, the enzyme NemR-PS with strict (*S*)-enantioselectivity in the reduction of (*E/Z*)-citral was engineered for activity improvement, making it necessary to avoid the trade-off effect between activity and enantioselectivity. The resulting NemR-PS variant together with alcohol dehydrogenase YsADH and glucose dehydrogenase BmGDH_{M6} was co-expressed in *E. coli*, serving as the whole-cell biocatalyst [16,17]. Various factors affecting cascade catalysis were investigated to enhance catalytic efficiency in one pot, two-step reduction of (*E/Z*)-citral to (*S*)-citronellol (Scheme 1). Finally, the substrate constant feeding was applied to increase the product accumulation and eliminate the residual intermediate and by-product.



Scheme 1. One pot, two-step reduction of (*E/Z*)-citral to (*S*)-citronellol using the *E. coli* cells co-expressing old yellow enzyme NemR-PS or its variants, alcohol dehydrogenase YsADH and glucose dehydrogenase BmGDH_{M6}.

2. Results and Discussion

2.1. Homologous Modeling and Alanine Scanning of NemR-PS

To perform the structure-guided engineering of NemR-PS, the structure model of NemR-PS was built on the basis of the structure of pentaerythritol tetranitrate reductase (PETNR) from *Enterobacter cloacae* PB2 (PDB ID: 3p62) [18]. Both NemR-PS and the template protein PETNR shared the sequence identity of 82% (Figure S1). In model evaluation, the results of both Verify-3D analysis and Ramachandran plot analysis indicated that the NemR-PS model was reliable (Figure S2). To identify the key residues on activity and enantioselectivity, molecular docking of NemR-PS and the ligand (*E*)-citral or (*Z*)-citral was performed using the program Autodock 4.2 (Figure 1). The active sites of NemR-PS contained a pair of residues His182/His185 as hydrogen bond donors for substrate electron-absorbing groups and a conserved residue Y187 (Figure S1) [19]. Taking the docked ligand as the center, the residues within 5 Å vicinity were considered as putative hot spots. Except the catalytic triad (His182, His185 and Y187), nine residues (F351, D275, F241, W103, Q242, R143, W276, S272 and Y352) were subjected to alanine scanning [20]. The resulting variants and the wild type NemR-PS were expressed in *E. coli* BL21(DE3) at the similar expression level (Figure S3). The cells expressing NemR-PS variants were collected and disrupted, and the evaluation was based on crude enzyme activity. Compared with the wild type NemR-PS, the specific activities of the variants F351A and D275A were increased by 48.90% and 41.80%, respectively (Figure 2). Thus, the residues F351 and D275 were chosen for subsequent site-saturation mutagenesis and iterative saturation mutation.

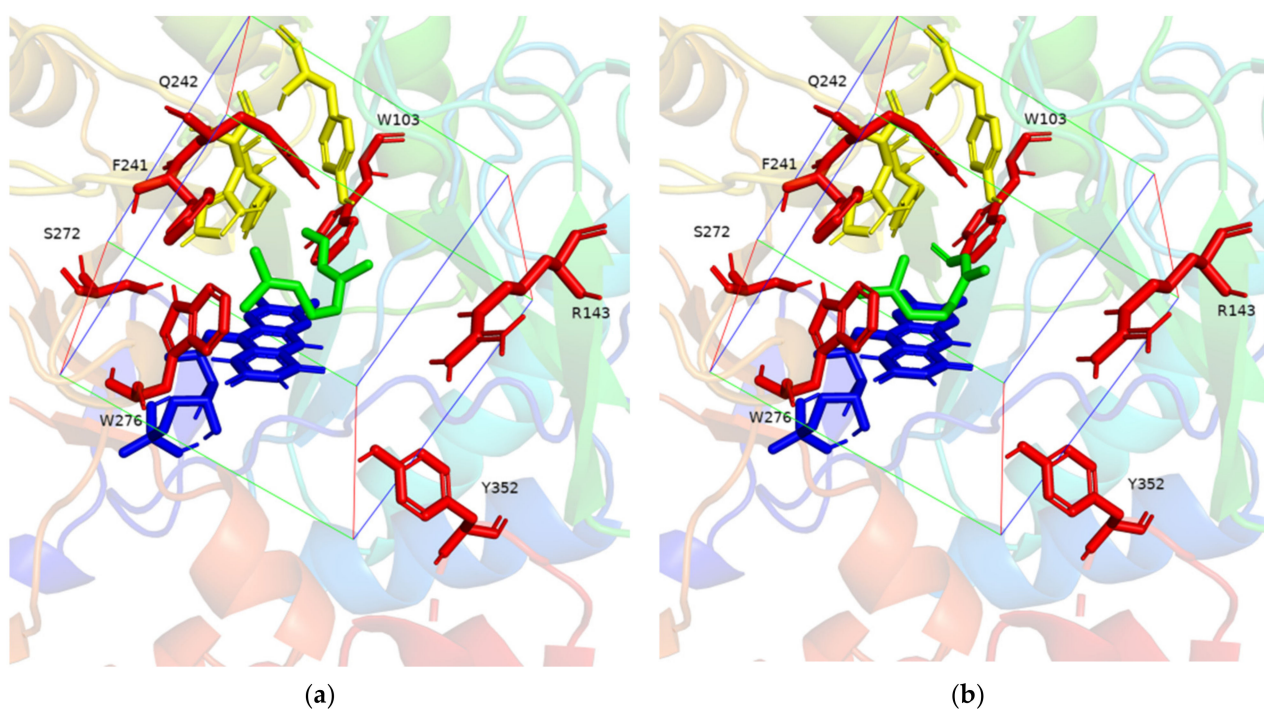
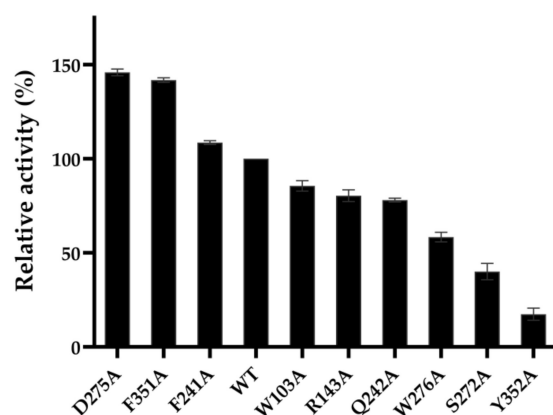


Figure 1. Identification of putative hot spots through molecular docking of NemR-PS and the ligand (*Z*)-citral (a) or (*E*)-citral (b). The box in the figure represents the 5 Å vicinity of the docked ligand as the center. Green, ligand; blue, cofactor FMN, yellow, active sites; red, putative hot spots.



NemR-PS and its variants

Figure 2. Crude enzyme activity of NemR-PS variants in alanine scanning. The assay mixture consisted of 100 μ g crude enzyme, 20 mM (*E/Z*)-citral, 0.4 mM NADPH and 100 mM PIPES buffer (pH 7.0). The activity was measured in triplicate at 30 °C by monitoring changes in the absorbance at 340 nm. The relative activity of 100% represents 0.34 U/mg.

2.2. Site-Saturation Mutagenesis of the Residue D275 and Iterative Saturation Mutagenesis of the Residue F351 in NemR-PS

To investigate the best substitution of the residue D275, site-directed saturation mutagenesis was performed and the resulting variants were expressed in *E. coli* at nearly the same level of expression (Figure S4). The substitution of D275 to aliphatic residue G, A, V, L or I caused significant activity improvement. Among them, the variant D275G (designated as M₁) was the most active and its crude enzyme activity reached up to 0.55 U/mg (Figure 3a). To investigate if the synergistic effect of the residues D275 and F351 existed, iterative saturation mutation of the residue F351 was further performed on the basis of D275G. Similarly, the resulting variants were successfully expressed in *E. coli* and the crude enzyme activity of each variant was determined for evaluation. The best variant D275G/F351A showed the specific activity of 0.86 U/mg, which was 2.32 times that of the wild type (Figure 3b). The engineering of NemR-PS aimed to not only improve the activity but also maintain its strict (*S*)-enantioselectivity. The enantioselectivity of all the variants from site-saturation mutagenesis and iterative saturation mutagenesis was determined through whole-cell catalyzed reduction of (*E/Z*)-citral to (*S*)-citronellal. All the tested variants exhibited strict (*S*)-enantioselectivity, indicating that the residues D275 and F351 had no negative effect on (*S*)-enantioselectivity.

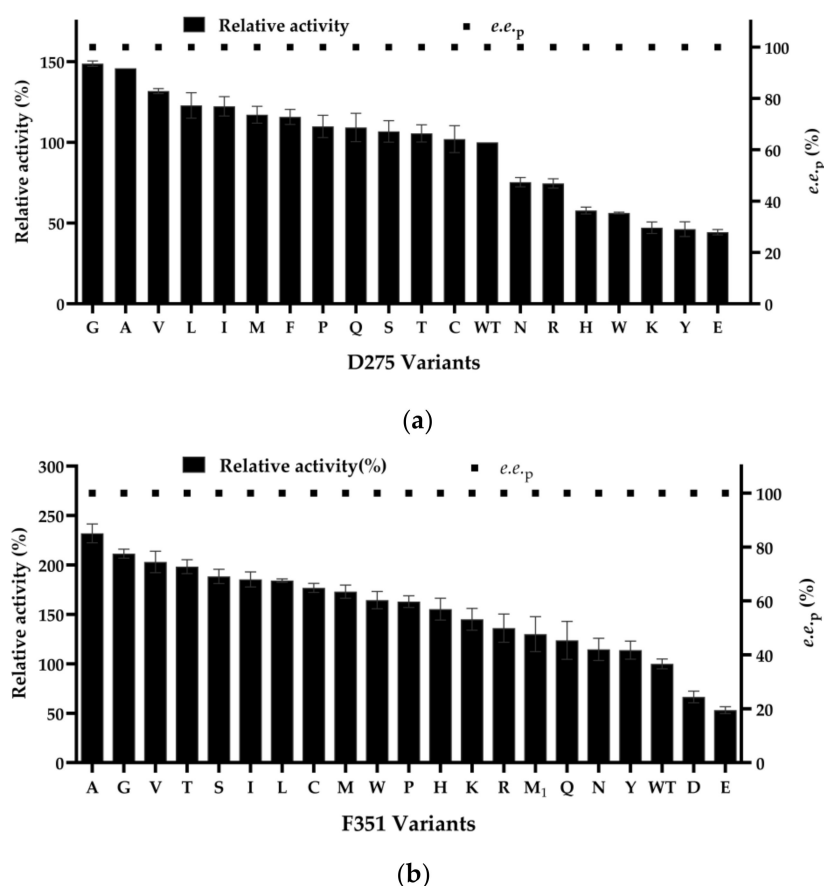


Figure 3. Activity (a) and enantioselectivity (b) of NemR-PS variants in site-saturation mutagenesis of the residue D275 and iterative saturation mutagenesis of the residue F351. (a), the assay mixture consisted of 100 μg crude enzyme, 20 mM (*E/Z*)-citral, 0.4 mM NADPH and 100 mM PIPES buffer (pH 7.0). The activity was measured in triplicate at 30 $^{\circ}\text{C}$ by monitoring changes in the absorbance at 340 nm. The relative activity of 100% represents 0.34 U/mg. (b), the reaction mixture consisted of 50 g/L wet cells expressing NemR-PS or its variants, 100 mM (*E/Z*)-citral, 300 mM glucose, 50 g/L wet cell expressing BmGDH_{M6}, 0.12 mM NADP⁺ and 50 mM PIPES buffer (pH 7.0). Constant pH was kept through the titration of 1 M NaOH. The reaction was run at 30 $^{\circ}\text{C}$ and 400 rpm for 2 h.

2.3. Kinetic Parameters of the Variant D275/F351A and Molecular Docking Analysis

To achieve accurate assessment of activity improvement, both NemR-PS and the variant D275/F351A were purified using Ni-NTA affinity chromatography. Obeying substrate inhibition kinetics, the kinetic parameters of NemR-PS and the variant D275/F351A were determined. The $K_{\text{cat}}/K_{\text{m}}$ value was increased from 2.09 $\text{s}^{-1}\text{mM}^{-1}$ of NemR-PS to 5.01 $\text{s}^{-1}\text{mM}^{-1}$ of the variant D275G/F351A (Table 1). Moreover, the double substitution endowed the rise of the K_{i} value from 39.79 mM to 128.50 mM, suggestion superior tolerance of the variant D275G/F351A to high concentration substrate.

Molecular docking analysis was further performed to gain an in-depth understanding of activity improvement. In the docking of NemR-PS and the substrate, Y187 and FMNH₂ contributed their hydrogen atoms to the C=C bond of citral, in which a hydrogen atom from FMNH₂ was enantioselectively transferred to the substrate C _{β} atom and the residue Y187 provided a proton to the substrate C _{α} atom. The activity improvement could be well explained by the variation of the distance from the hydroxyl group of Y187 to the C _{α} atom of the substrate (D1) and the distance from the N₅ atom of FMNH₂ to the C _{β} atom of the substrate (D2) [19,21,22]. When the substrate (*Z*)-citral was docked, the double substitution of D275G/F351A changed the values of D1 and D2 from 3.4 \AA and 3.3 \AA to 3.1 \AA and 2.7 \AA , respectively (Figure 4a,c). Similarly, decreasing values of D1 and D2 were observed

when (*Z*)-citral was replaced by (*E*)-citral in the docking model (Figure 4b,d). In addition, molecular docking analysis of both NemR-PS and the variant D275G/F351A indicated that the binding mode of (*Z*)-citral or (*E*)-citral led to the same (*S*)-configuration in the enantioselective hydrogenation of the C_β atom of the substrate, which was consistent with strict (*S*)-enantioselectivity in the reduction of (*E/Z*)-citral.

Table 1. Kinetic parameters of the purified NemR-PS and NemR-PS-D275G/F351A¹.

	NemR-PS	NemR-PS-D275G/F351A
K_i (mM)	39.79 ± 1.23	128.50 ± 1.23
V_{max} (U/mg)	1.98 ± 0.11	2.64 ± 0.15
K_m (mM)	0.63 ± 0.13	0.35 ± 0.08
K_{cat} (s ⁻¹)	1.32 ± 0.07	1.75 ± 0.10
K_{cat}/K_m (s ⁻¹ mM ⁻¹)	2.09 ± 0.11	5.01 ± 0.28

¹ The assay mixture consisted of 7 μg purified enzyme, 0.2–100 mM (*E/Z*)-citral, 0.4 mM NADPH and 100 mM PIPES buffer (pH 7.0). The activity was measured in triplicate at 30 °C by monitoring changes in the absorbance at 340 nm. According to the substrate inhibition kinetics, apparent values of K_m , K_i and V_{max} were calculated using curve fitting from software Prism 8 (GraphPad Software, San Diego, CA, USA).

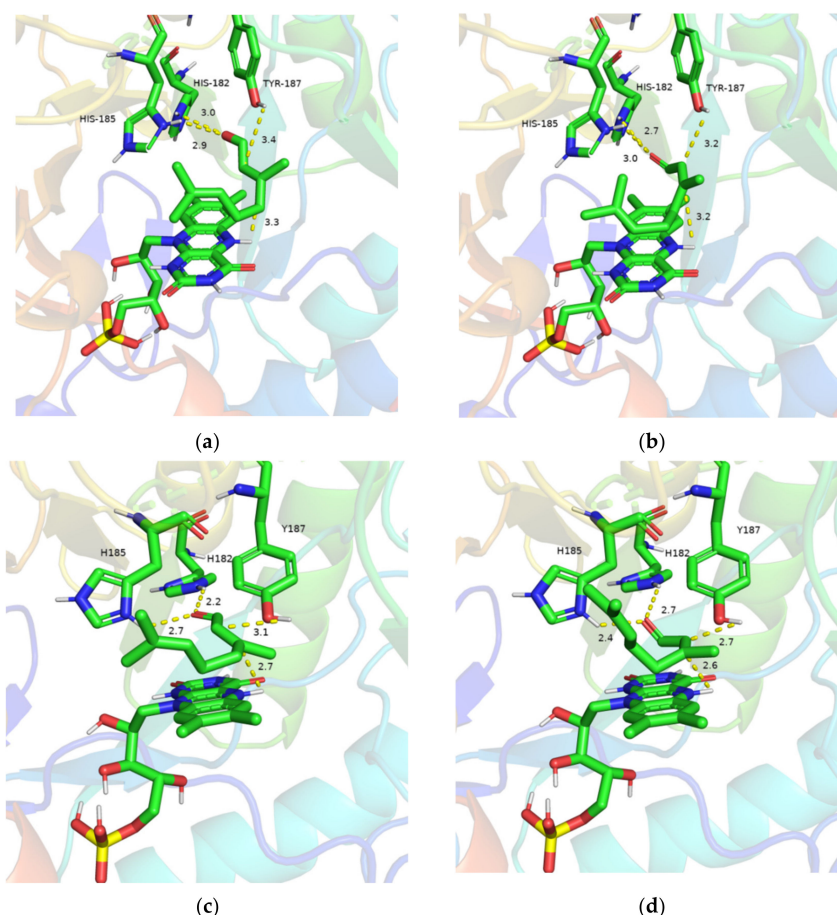


Figure 4. Molecular docking of old yellow enzyme (NemR-PS or its variant D275G/F351A) and the substrate (*Z*)-citral or (*E*)-citral. (a), NemR-PS and (*Z*)-citral; (b), NemR-PS and (*E*)-citral; (c), NemR-PS variant D275G/F351A and (*Z*)-citral; (d), NemR-PS variant D275G/F351A and (*E*)-citral. Green, carbon atom; blue, nitrogen atom; tangerine, oxygen atom; white, hydrogen atom; yellow, phosphorus atom.

2.4. Key Factors Affecting Whole-Cell Catalyzed Reduction of (*E/Z*)-Citral to (*S*)-Citronellol

The old yellow enzyme NemR-PS D275G/F351A together alcohol dehydrogenase YsADH and glucose dehydrogenase BmGDH_{M6} was cascaded for one-pot, two-step reduc-

tion of (*E/Z*)-citral to (*S*)-citronellol. In order to overcome the diffusion restriction of substrates between cell membranes [13], the whole-cell catalyst *E. coli* BL21(DE3)/pACYCDuet-1-*YsADH*-*BmGDH*_{M6}/pET28a-*NemR-PS-D275G/F351A* was constructed to co-express *YsADH*, *BmGDH*_{M6} and *NemR-PS D275G/F351A* (Figure S7). The co-expression of *YsADH*, *BmGDH*_{M6} and *NemR-PS D275G/F351A* were verified by the determination of crude enzyme activity, which specific activities corresponded to 0.79 U/mg, 0.36 U/mg and 0.79 U/mg, respectively. The key parameters for whole-cell catalyzed reduction of (*E/Z*)-citral to (*S*)-citronellol were optimized to be 30 °C, pH 6.5, 400 rpm and 0.4 mM NADP⁺, which were the same as the previously-reported procedure [7]. The optimal ratio of substrate to co-substrate glucose was determined to be 1:3 (Figure 5a). In addition, the addition of 4% (*v/v*) isopropanol as co-solvent exhibited the highest product yield (Figure 5b).

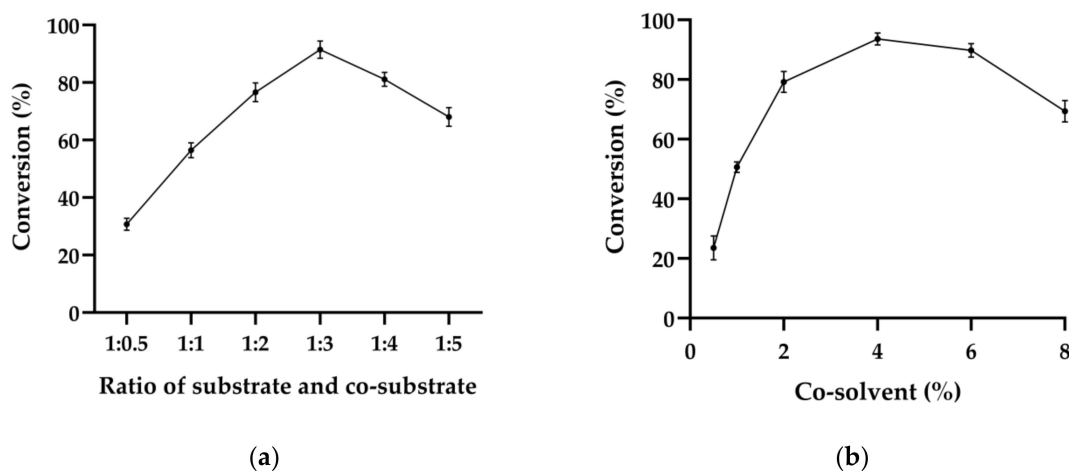


Figure 5. Effect of co-substrate (a) and co-solvent (b) on two-step reduction of (*E/Z*)-citral to (*S*)-citronellol. (a), the reaction mixture (10 mL) contained 100 g/L wet cells co-expressing three enzymes, 300 mM (*E/Z*)-citral, 150~1500 mM glucose, 0.4 mM NADP⁺, 4% (*v/v*) isopropanol and 50 mM PIPES buffer (pH 6.5). (b), the reaction mixture (10 mL) contained 100 g/L wet cells expressing three enzymes, 300 mM (*E/Z*)-citral, 900 mM glucose, 0.4 mM NADP⁺, 0.5~8% (*v/v*) isopropanol and 50 mM PIPES buffer (pH 6.5). Constant pH was kept through the titration of 1 M NaOH. The reactions were conducted at 30 °C and 400 rpm for 12 h. Standard deviations are indicated in the diagram ($n = 3$).

Under the optimized conditions, the biotransformation of 300 mM in 12 h led to the conversion of 95.13%. To investigate the formation of intermediate and by-product, the substrate concentration was set as 400 mM when the time courses of one pot, two-step reduction of (*E/Z*)-citral to (*S*)-citronellol were depicted (Figure 6). As the substrate was consumed, the product gradually accumulated within the 12 h reaction. The by-products included predominant geraniol and minor nerol from alcohol dehydrogenase-catalyzed reduction of (*E*)-citral and (*Z*)-citral, reflecting that the old yellow enzyme had higher activity toward (*Z*)-citral than (*E*)-citral. The intermediate was the sole (*S*)-citronellal, supporting that *NemR-PS D275G/F351A*-catalyzed reduction of both (*E*)-citral and (*Z*)-citral led to the same (*S*)-citronellal. In the first 4 h reaction, the by-product geraniol and the intermediate (*S*)-citronellal accumulated. During the reaction from 4 h to 12 h, the by-product geraniol was dehydrogenated to return the pool of the substrate while the intermediate (*S*)-citronellal was completely converted to the product (*S*)-citronellol. The conversion after 12 h cascade reaction was 89.16%. Compared with the whole-cell biocatalyst co-expressed *NemR-PS*, the whole-cell biocatalyst co-expressed *NemR-PS D275G/F351A* shortened the reaction time from 36~48 h to 12 h [7], suggesting that activity improvement of the old yellow enzyme significantly enhanced the catalytic efficiency of cascade catalysis. When the reaction was extended to 24 h, the concentration of (*S*)-citronellol has no substantial

increase and the conversion of geraniol remained around 10%, suggesting that at least one of the enzymes did not function well against 400 mM substrate.

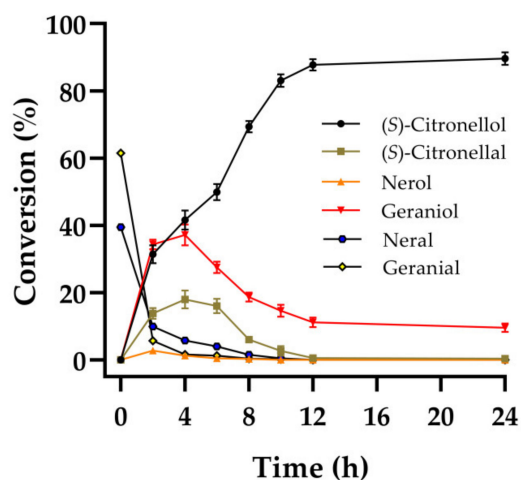


Figure 6. Time courses of the reduction of 400 mM (*E/Z*)-citral to (*S*)-citronellol. The reaction mixture (10 mL) contained 100 g/L wet cells co-expressing three enzymes, 400 mM (*E/Z*)-citral, 1200 mM glucose, 0.4 mM NADP⁺, 4% (*v/v*) isopropanol and 50 mM PIPES buffer (pH 6.5). Constant pH was kept through the titration of 1 M NaOH. The reactions were conducted at 30 °C and 400 rpm for 24 h. Standard deviations are indicated in the diagram ($n = 3$).

2.5. Synthesis of (*S*)-Citronellol in the Manner of Substrate Constant Feeding

Although the double substitution D275G/F351A increased the kinetic parameter K_i from 39.79 to 128.50 mM, it was speculated that higher substrate concentration (e.g., 400 mM) would cause severe inhibition on the activity of the variant. As an α,β -unsaturated aldehyde, (*E/Z*)-citral could form covalent interaction with the lysine and cysteine residues of old yellow enzyme, alcohol dehydrogenase and/or glucose dehydrogenase, resulting in the decreasing activity [23]. Substrate batch or constant feeding is an easy-to-use way to relieve the substrate inhibition [15,24]. Here, the loadings of 500 mM (*E/Z*)-citral and 1500 mM glucose were pumped into 10 mL reaction system at a constant flow rate within 10 h. The product concentration in the reaction system rose synchronously with the flow of the substrate (Figure 7). After 10 h of the reaction, there were minor amounts of by-product geraniol and intermediate (*S*)-citronellal, which were completely converted to the product in the next 2 h. The product in the reaction mixture was verified to be (*S*)-citronellol by a combination of GC and GC-mass spectrometry (GC-MS) (Figure S9 and S10). The substrate constant feeding strategy increased the product accumulation up to 500 mM and avoided the accumulation of by-product and intermediate, suggesting that it was an effective way to relieve the substrate inhibition.

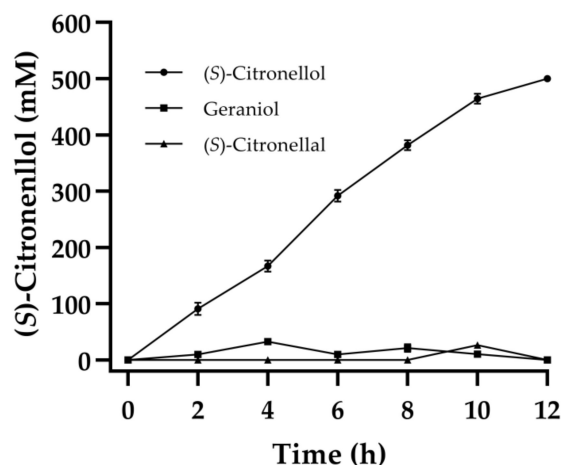


Figure 7. The synthesis of (*S*)-citronellol in the manner of substrate constant feeding. The initial reaction mixture (10 mL) contains 100 g/L wet cells co-expressing three enzymes, 0.4 mM NADP⁺, 4% (*v/v*) isopropanol and 50 mM PIPES buffer (pH 6.5). The loading of 500 mM substrate and 1500 mM glucose was constantly fed within 10 h. The reaction was performed at 30 °C and 400 rpm for 12 h. Constant pH was kept through the titration of 1 M NaOH. Standard deviations are indicated in the diagram ($n = 3$).

3. Materials and Methods

3.1. Chemicals, Genes and Organisms

The standard chemicals were purchased from Sigma-Aldrich (Shanghai, China) and common chemicals were commercially available. Restriction enzymes, DNA polymerase and the kits for gene manipulation were bought from Takara Biomedical Technology Co., Ltd. (Beijing, China) and Vazyme Biotech Co., Ltd. (Nanjing, China). Materials for protein purification was purchased from GE Healthcare Life Sciences (Shanghai, China).

Primers and synthesized genes were obtained from Tsingke Biotechnology Co., Ltd. (Hangzhou, China). The plasmids pET28a and pACYCDuet-1 together with the strain *E. coli* BL21 (DE3) were used for constructing recombinant strains co-expressing old yellow enzyme, alcohol dehydrogenase and glucose dehydrogenase.

3.2. Expression and Purification of NemR-PS

The gene encoding NemR-PS was inserted into the *Nco* I/*Xho* I site of the vector pET28a and the resulting plasmid was transferred into *E. coli* BL21(DE3), offering the recombinant strain *E. coli* BL21(DE3)/pET28a-NemR-PS. The recombinant strain was initially grown at 37 °C in LB medium containing 50 µg/mL kanamycin. When the OD₆₀₀ value was 0.6, 0.2 mM isopropyl-β-D-thiolactopyranoside (IPTG) was added to induce NemR-PS expression at 24 °C for 12 h. After induction, the cells were harvested by centrifugation at 4 °C for 10 min. Similarly, the strain *E. coli* BL21 (DE3)/pET28a-BmGDH_{M6} was successfully constructed to express BmGDH_{M6}.

The cells expressing NemR-PS were re-suspended in 50 mM Tris HCl buffer (pH 8.0) and disrupted by sonication for 10 min. After centrifugation, the cell debris pellets were discarded and the cell-free extracts were applied for Ni-NTA chelating affinity chromatography. Unbound proteins were washed off by applying the binding buffer (5 mM imidazole and 300 mM NaCl dissolved in 50 mM Tris-HCl, pH 8.0), whereas NemR-PS was eluted out by applying the elution buffer (200 mM imidazole and 300 mM NaCl dissolved in 50 mM Tris-HCl, pH 8.0). The purity of the purified enzyme was verified using sodium dodecyl sulfate-polyacrylamide gel electrophoresis (SDS-PAGE) as described previously [25]. The purified NemR-PS samples were desalted with 50 mM Tris-HCl buffer (pH 8.0) and stored at −20 °C for further investigation.

3.3. Homology Modeling and Molecular Docking

The structural model of NemR-PS was built on the AI-aided web server iDrug (<https://drug.ai.tencent.com>, accessed on 1 July 2021), using the crystal structure of the old yellow enzyme PETNR (PDB ID: 3P62) as template. The model was evaluated by Ramachandran plots and Verify-3D. (*E*)-Citral or (*Z*)-citral as ligand was docked with NemR-PS using AutoDock 4.2 program (The Scripps Research Institute, La Jolla, CA, USA) [26]. The optimal configuration and resulting substrate-enzyme complex were further processed using the PyMOL software (The PyMOL Molecular Graphics System, Version 2.0 Schrödinger, LLC.) [27].

3.4. Site-Directed/Saturation Mutagenesis of NemR-PS

Following the whole-plasmid mutagenesis protocol [28], site-directed/saturation mutagenesis of NemR-PS was run using the recombinant plasmid pET28a-NemR-PS as template. The PCR reaction mixture (50 μ L) consisted of 1 μ L forward primer (110 μ M), 1 μ L reverse primer (110 μ M), 25 μ L 2 \times buffer, 1 μ L dNTP mixture (each 10 mM), 1 μ L plasmid template, 1 μ L DNA Polymerase, and 20 μ L water. The primers for site-directed/saturation mutagenesis was listed in Table S1–S3. The PCR conditions: 95 $^{\circ}$ C for 5 min, and then 30 cycles (95 $^{\circ}$ C for 15 s, 55–61 $^{\circ}$ C for 15 s, 72 $^{\circ}$ C for 1 min), 72 $^{\circ}$ C extension for 5 min. In iterative saturation mutagenesis, the recombinant plasmid pET28a-NemR-PS-D275G was used as template. The PCR products was digested by *Dpn* I at 37 $^{\circ}$ C for 1 h and then directly transformed into *E. coli* BL21(DE3) competent cells to generate the variants. The induction and purification of the resulting NemR-PS variant was run using the same procedure as NemR-PS in Section 3.2.

3.5. Activity Assay and Determination of Kinetic Parameters

The crude enzyme activities of alcohol dehydrogenase, old yellow enzyme and glucose dehydrogenase were measured at 30 $^{\circ}$ C by monitoring changes in absorbance at 340 nm. All enzyme assays were performed in triplicate. The 200 μ L assay mixture of old yellow enzyme consisted of 100 μ g crude enzyme, 20 mM citral, 0.4 mM NADPH and 50 mM PIPES buffer (pH 7.0). The 200 μ L assay mixture of alcohol dehydrogenase consisted of 100 μ g crude enzyme, 20 mM citronellal, 0.4 mM NADPH and 50 mM PIPES buffer (pH 7.0). The 200 μ L assay mixture for glucose dehydrogenase contains 100 μ g crude enzyme, 20 mM glucose, 0.4 mM NADP⁺ and 50 mM PIPES buffer (pH 7.0). The enzyme assays began with the addition of the coenzyme NADPH or NADP⁺. One unit of activity represents the formation or oxidation of 1 μ mol NADPH per minute. The BCA method was used to determine the protein concentration of all samples as well as bovine serum albumin as the standard protein [29].

In the determination of kinetic parameters, the 200 μ L assay mixture consisted of 7 μ g purified enzyme, various concentrations of citral (0.2, 0.5, 1, 2, 5, 10, 20, 50 and 100 mM), 0.4 mM NADPH and 50 mM PIPES buffer (pH 7.0). The activity was measured in triplicate at 30 $^{\circ}$ C by monitoring changes in the absorbance at 340 nm. According to substrate inhibition kinetics, apparent values of K_m , K_i and V_{max} were calculated using curve fitting from software Prism 8 (GraphPad Software, San Diego, CA, USA).

3.6. Determination of Enantiomeric Excess Value of NemR-PS and Its Variants

To determine enantioselectivity of NemR-PS and its variants, the strain expressing NemR-PS and that expressing BmGDH_{M6} were used as biocatalyst to catalyze the reduction of (*E/Z*)-citral to (*S*)-citronellal, respectively. The reaction mixture (10 mL) contains 100 mM (*E/Z*)-citral, 300 mM glucose, 50 g/L wet cells expressing NemR-PS or its variants, 50 g/L wet cells expressing BmGDH_{M6} and 50 mM PIPES buffer (pH 7.0). The reaction was performed at 30 $^{\circ}$ C and 400 rpm for 2 h. The reaction mixture was extracted with 4 volumes of ethyl acetate. After extraction, the organic phase was collected through centrifugation at 8000 \times g for 10 min and dehydrated with anhydrous sodium sulfate. Finally, 1 μ L of

dehydrated sample was injected for GC analysis using previously-reported parameters [7] (Figure S9).

3.7. Co-Expression of *YsADH*, *NemR-PS-D275G/F351A* and *BmGDH_{M6}*

The gene encoding *YsADH* was amplified using a pair of primers pET28a-*YsADH*-F and pET28a-*YsADH*-R (Table S4). The PCR program consisted of the following steps: 98 °C for 5 min, 30 cycles (98 °C for 10 s, 58 °C for 15 s, and 72 °C for 30 s), and 72 °C extension for 5 min. Linear pACYCDuet-1 fragments were amplified by reverse PCR using primers pACYCDuet-1-F and pACYCDuet-1-R (Table S4). The corresponding PCR procedure was as follows: 98 °C for 5 min, 30 cycles (98 °C for 10 s, 58 °C for 15 s, and 72 °C for 90 s), and 72 °C extension for 5 min. According to the instructions of the ClonExpress MultiS one-step cloning kit (Vazyme Biotech Co., Ltd., Nanjing, China), the gene encoding *YsADH* was connected with the linear pACYCDuet-1 fragment through homologous recombinant ligation derived from Exnase II to form the recombinant plasmid pACYCDuet-1-*YsADH*. Similarly, the gene encoding *BmGDH_{M6}* was introduced into the plasmid pACYCDuet-1-*YsADH* to form the recombinant plasmid pACYCDuet-1-*YsADH*-*BmGDH_{M6}*. The primers used to construct the plasmid pACYCDuet-1-*YsADH*-*BmGDH_{M6}* were listed in Table S5. In the plasmid pACYCDuet-1-*YsADH*-*BmGDH_{M6}*, the genes encoding *YsADH* and *BmGDH_{M6}* were located between the sites of *Nco* I/*Hind* III and *Nde* I/*Xho* I, respectively. The plasmid pACYCDuet-1-*YsADH*-*BmGDH_{M6}* was transformed into the strain *E. coli* BL21(DE3)/pET28a-*NemR-PS-D275G/F351A*, offering the recombinant strain *E. coli* BL21(DE3)/pACYCDuet-1-*YsADH*-*BmGDH_{M6}*/pET28a-*NemR-PS-D275G/F351A*. The wet cells co-expressing old yellow enzyme, alcohol dehydrogenase and glucose dehydrogenase were induced and collected for further use, according to the procedure described in Section 3.2.

3.8. Key Factors on Double Reduction of (*E/Z*)-Citral to (*S*)-Citronellol

The reduction of (*E/Z*)-citral to (*S*)-citronellol was catalyzed by the strain *E. coli* BL21(DE3)/pACYCDuet-1-*YsADH*-*BmGDH_{M6}*/pET28a-*NemR-PS-D275G/F351A* as biocatalyst. The initial reaction mixture (10 mL) contains 300 mM (*E/Z*)-citral, 900 mM glucose, 100 g/L wet cells, 0.4 mM NADP⁺ and 50 mM PIPES buffer (pH 6.5). Before optimized, the initial reaction conditions are 30 °C and 200 rpm for 12 h. The pH value was kept constant by using an automatic titration of 1 M NaOH. These factors varied individually to test its effect on the reduction of (*E/Z*)-citral to (*S*)-citronellol. The optimal temperature was explored by changing the temperature from 20 °C to 45 °C. Optimal pH values were studied in the pH range of 5.5 to 8.0. The buffers used are citrate (pH 5.0 and 5.5), PIPES (pH 6.0, 6.5 and 7.0) and Tris-HCl (pH 7.5 and 8.0). The rotation was explored in the range of 200 to 700 rpm. The concentration of NADP⁺ was tested in the range of 0 to 1.0 mM. The ratio of substrate to co-substrate was selected in the range of 1:0.5–1:5. The co-solvent isopropanol was tested by varying from 0.5% to 8% (*v/v*).

3.9. Time Courses of the Reduction of 400 mM Citronellol to (*S*)-Citronellol

To elucidate the dynamic changes of substrate, product, by-product and intermediate, the time courses of the reduction of 400 mM (*E/Z*)-citral were explored by sampling every 2 h. The reaction mixture (10 mL) contained 400 mM (*E/Z*)-citral, 1200 mM glucose, 100 g/L wet cells co-expressing three enzymes, 0.4 mM NADP⁺, 4% (*v/v*) isopropanol and 50 mM PIPES buffer (pH 6.5). Constant pH was kept by the automatic titration of 1 M NaOH. The reaction was performed at 30 °C and 400 rpm for 24 h. The reaction mixture was extracted with 4 volumes of ethyl acetate. After extraction, the organic phase was collected through centrifugation, dehydrated with anhydrous sodium sulfate and subjected for GC analysis using previously-reported parameters (Figure S9) [7]. Citral, citronellal and citronellol were validated through GC-MS analysis (Agilent7890A/5975C, Agilent Technologies Inc., Santa Clara, CA, USA) using previously-reported parameters (Figure S10) [30].

3.10. Synthesis of (S)-Citronellol in the Manner of Substrate Constant Feeding

The initial reaction mixture (10 mL) contained 100 g/L wet cells co-expressing three enzymes, 0.4 mM NADP⁺, 4% (*v/v*) isopropanol and 50 mM PIPES buffer (pH 6.5). Using a syringe pump, the loadings of 500 mM (*E/Z*)-citral and 1500 mM glucose were constantly fed within 10 h. The reaction was performed at 30 °C and 400 rpm for 12 h. In the entire reaction, constant pH was kept through the automatic titration of 1 M NaOH. Following the same procedure described in Section 3.9, the substrate, intermediate, product and by-product were extracted and then subjected for GC and GC–MS analyses.

4. Conclusions

The combinatorial efforts of protein engineering, biocatalyst engineering and process engineering significantly enhanced the catalytic efficiency in the reduction of (*E/Z*)-citral to (*S*)-citronellol. Firstly, the semi-rational design on the substrate binding pocket of the enzyme NemR-PS led to the activity-improved variant D275G/F351A, which K_{cat}/K_m value ($5.01 \text{ s}^{-1}\text{mM}^{-1}$) was 2.40 times higher than that of the wild type ($2.09 \text{ s}^{-1}\text{mM}^{-1}$). Obeying the substrate inhibition kinetics, the double substitution D275G/F351A increased the K_i value from 39.79 mM to 128.50 mM, endowing superior tolerance to high concentration substrate. The variant D275G/F351A possessed the same strict (*S*)-enantioselectivity as the wild type, avoiding the trade-off effect between activity and enantioselectivity. Then, the strain co-expressing old yellow enzyme NemR-PS D275G/F351A, alcohol dehydrogenase YsADH and glucose dehydrogenase BmGDH_{M6} was constructed to catalyze one-pot, two-step reduction of (*E/Z*)-citral to (*S*)-citronellol. In the whole-cell system, various factors affecting the cascade catalysis were explored. Finally, the substrate constant feeding was applied to completely eliminate the residual intermediate and by-product. Compared with our previous study [7], the newly-developed methodology increased not only the accumulation of the product up to 500 mM but also shortened the reaction time from 36–48 h to 12 h.

Supplementary Materials: The following supporting information can be downloaded at: <https://www.mdpi.com/article/10.3390/catal12060631/s1>, Table S1: The primers for alanine scanning in NemR-PS; Table S2: The primers for saturation mutagenesis of the residue D275 in NemR-PS; Table S3: The primers for iterative saturation mutagenesis of the residue F351 in NemR-PS D275G; Table S4: The primers for constructing the recombinant plasmid pACYCDuet-1-YsADH; Table S5: The primers for constructing the recombinant plasmid pACYCDuet-1-YsADH-BmGDH_{M6}; Figure S1: Sequence comparison of old yellow enzymes PETNR and NemR-PS; Figure S2: The model evaluation through the Verify-3D analysis (a) and the Ramachandran plot (b); Figure S3: SDS-PAGE analysis of NemR-PS variants in alanine scanning; Figure S4: SDS-PAGE analysis of NemR-PS variants in site-saturation mutagenesis of the residue D275; Figure S5: SDS-PAGE analysis of NemR-PS variants in iterative site-saturation of D275G and the residue F351; Figure S6: SDS-PAGE analysis of the purified NemR-PS and its variant D275G/F351A; Figure S7: SDS-PAGE analysis of the strain co-expressing co-expressing NemR-PS D275G/F351A, YsADH and BmGDH_{M6}; Figure S8: Factors affecting the reduction of (*E/Z*)-citral to (*S*)-citronellol; Figure S9: GC analyses of substrate, intermediate, product and by-products; Figure S10: The GC-MS analyses of substrate, intermediate and product.

Author Contributions: Conceptualization, Y.Z. and X.Y.; methodology, software, validation, formal analysis, investigation, resources, data curation, B.F., X.L., L.J., Y.W., Y.T., Y.H., C.L., J.S., Y.Z. and X.Y.; writing—original draft preparation, B.F. and X.Y.; writing—review and editing, B.F., X.L., L.J., Y.W., Y.T., Y.H., C.L., J.S., Y.Z. and X.Y.; visualization, X.Y.; supervision, Y.Z. and X.Y.; project administration, Y.Z. and X.Y.; funding acquisition, Y.Z. All authors have read and agreed to the published version of the manuscript.

Funding: This research was supported by Key Projects of Technological Innovation and Application Development of Chongqing City, China (No. cstc2021jscx-jbgs X0002) and The Natural Science Foundation of Zhejiang Province, China (No. LY18B020021).

Data Availability Statement: The data presented in this study are available in Supplementary Material.

Conflicts of Interest: The authors declare no conflict of interest.

References

1. Santos, P.L.; Matos, J.; Picot, L.; Almeida, J.; Quintans, J.S.S.; Quintans-Junior, L.J. Citronellol, a monoterpene alcohol with promising pharmacological activities—A systematic review. *Food Chem. Toxicol.* **2019**, *123*, 459–469. [[CrossRef](#)]
2. Majumder, A.B.; Shah, S.; Gupta, M.N. Enantioselective transacetylation of (*R,S*)-beta-citronellol by propanol rinsed immobilized *Rhizomucor miehei* lipase. *Chem. Cent. J.* **2007**, *1*, 10. [[CrossRef](#)] [[PubMed](#)]
3. Yamamoto, T.; Matsuda, H.; Utsumi, Y.; Hagiwara, T.; Kanisawa, T. Synthesis and odor of optically active rose oxide. *Tetrahedron Lett.* **2002**, *43*, 9077–9080. [[CrossRef](#)]
4. Mäki-Arvela, P.; Tiainen, L.P.; Lindblad, M.; Demirkan, K.; Kumar, N.; Sjöholm, R.; Ollonqvist, T.; Väyrynen, J.; Salmi, T.; Murzin, D.Y. Liquid-phase hydrogenation of citral for production of citronellol: Catalyst selection. *Appl. Catal. A* **2003**, *241*, 271–288. [[CrossRef](#)]
5. Yu, W.; Liu, H.; Liu, M.; Liu, Z. Selective hydrogenation of citronellal to citronellol over polymer-stabilized noble metal colloids. *React. Funct. Polym.* **2000**, *44*, 21–29. [[CrossRef](#)]
6. Ribeaucourt, D.; Bissaro, B.; Lambert, F.; Lafond, M.; Berrin, J.G. Biocatalytic oxidation of fatty alcohols into aldehydes for the flavors and fragrances industry. *Biotechnol. Adv.* **2022**, *56*, 107787. [[CrossRef](#)]
7. Jia, Y.; Wang, Q.; Qiao, J.; Feng, B.; Zhou, X.; Jin, L.; Feng, Y.; Yang, D.; Lu, C.; Ying, X. Cascading old yellow enzyme, alcohol dehydrogenase and glucose dehydrogenase for selective reduction of (*E/Z*)-citral to (*S*)-citronellol. *Catalysts* **2021**, *11*, 13. [[CrossRef](#)]
8. Hummel, W.; Groger, H. Strategies for regeneration of nicotinamide coenzymes emphasizing self-sufficient closed-loop recycling systems. *J. Biotechnol.* **2014**, *191*, 22–31. [[CrossRef](#)]
9. Zheng, L.; Lin, J.; Zhang, B.; Kuang, Y.; Wei, D. Identification of a yeast old yellow enzyme for highly enantioselective reduction of citral isomers to (*R*)-citronellal. *Bioresour. Bioprocess.* **2018**, *5*, 9. [[CrossRef](#)]
10. Amato, E.D.; Stewart, J.D. Applications of protein engineering to members of the old yellow enzyme family. *Biotechnol. Adv.* **2015**, *33*, 624–631. [[CrossRef](#)]
11. Bougioukou, D.J.; Kille, S.; Taglieber, A.; Reetz, M.T. Directed evolution of an enantioselective enoate-reductase: Testing the utility of iterative saturation mutagenesis. *Adv. Synth. Catal.* **2009**, *351*, 3287–3305. [[CrossRef](#)]
12. Zhang, B.; Du, H.; Zheng, Y.; Sun, J.; Shen, Y.; Lin, J.; Wei, D. Design and engineering of whole-cell biocatalyst for efficient synthesis of (*R*)-citronellal. *Microb. Biotechnol.* **2022**, *15*, 1486–1498. [[CrossRef](#)]
13. Daugelavicius, R.; Bakiene, E.; Bamford, D.H. Stages of polymyxin B interaction with the *Escherichia coli* cell envelope. *Antimicrob. Agents Chemother.* **2000**, *44*, 2969–2978. [[CrossRef](#)]
14. Sheldon, R.A.; Woodley, J.M. Role of biocatalysis in sustainable chemistry. *Chem. Rev.* **2018**, *118*, 801–838. [[CrossRef](#)]
15. Boodhoo, K.V.K.; Flickinger, M.C.; Woodley, J.M.; Emanuelsson, E.A.C. Bioprocess intensification: A route to efficient and sustainable biocatalytic transformations for the future. *Chem. Eng. Process.* **2022**, *172*, 108793. [[CrossRef](#)]
16. Ying, X.; Wang, Y.; Xiong, B.; Wu, T.; Xie, L.; Yu, M.; Wang, Z. Characterization of an allylic/benzyl alcohol dehydrogenase from *Yokenella* sp. strain WZY002, an organism potentially useful for the synthesis of α,β -unsaturated alcohols from allylic aldehydes and ketones. *Appl. Environ. Microbiol.* **2014**, *80*, 2399–2409. [[CrossRef](#)]
17. Qian, W.Z.; Ou, L.; Li, C.X.; Pan, J.; Xu, J.H.; Chen, Q.; Zheng, G.W. Evolution of glucose dehydrogenase for cofactor regeneration in bioredox processes with denaturing agents. *Chembiochem* **2020**, *21*, 2680–2688. [[CrossRef](#)]
18. Hulley, M.E.; Toogood, H.S.; Fryszkowska, A.; Mansell, D.; Stephens, G.M.; Gardiner, J.M.; Scrutton, N.S. Focused directed evolution of pentaerythritol tetranitrate reductase by using automated anaerobic kinetic screening of site-saturated Libraries. *ChemBioChem* **2010**, *11*, 2433–2447. [[CrossRef](#)]
19. Iorgu, A.I.; Baxter, N.J.; Cliff, M.J.; Waltho, J.P.; Hay, S.; Scrutton, N.S. ^1H , ^{15}N and ^{13}C backbone resonance assignments of pentaerythritol tetranitrate reductase from *Enterobacter cloacae* PB2. *Biomol. NMR Assign.* **2017**, *12*, 79–83. [[CrossRef](#)]
20. Morrison, K.L.; Weiss, G.A. Combinatorial alanine-scanning. *Curr. Opin. Chem. Biol.* **2001**, *5*, 302–307. [[CrossRef](#)]
21. Fryszkowska, A.; Toogood, H.; Sakuma, M.; Gardiner, J.M.; Stephens, G.M.; Scrutton, N.S. Asymmetric reduction of activated alkenes by pentaerythritol tetranitrate reductase: Specificity and control of stereochemical outcome by reaction optimisation. *Adv. Synth. Catal.* **2009**, *351*, 2976–2990. [[CrossRef](#)]
22. Iorgu, A.I.; Hedison, T.M.; Hay, S.; Scrutton, N.S. Selectivity through discriminatory induced fit enables switching of NAD(P)H coenzyme specificity in Old Yellow Enzyme ene-reductases. *FEBS J.* **2019**, *286*, 3117–3128. [[CrossRef](#)]
23. Dick, M.; Hartmann, R.; Weiergraber, O.H.; Bisterfeld, C.; Classen, T.; Schwarten, M.; Neudecker, P.; Willbold, D.; Pietruszka, J. Mechanism-based inhibition of an aldolase at high concentrations of its natural substrate acetaldehyde: Structural insights and protective strategies. *Chem. Sci.* **2016**, *7*, 4492–4502. [[CrossRef](#)]
24. Zhao, M.; Gao, L.; Zhang, L.; Bai, Y.; Chen, L.; Yu, M.; Cheng, F.; Sun, J.; Wang, Z.; Ying, X. Asymmetric reduction of ketopantolactone using a strictly (*R*)-stereoselective carbonyl reductase through efficient NADPH regeneration and the substrate constant-feeding strategy. *Biotechnol. Lett.* **2017**, *39*, 1741–1746. [[CrossRef](#)]
25. Laemmli, U.K. Cleavage of structural proteins during the assembly of the head of bacteriophage T4. *Nature* **1970**, *227*, 680–685. [[CrossRef](#)]
26. Morris, G.M.; Huey, R.; Lindstrom, W.; Sanner, M.F.; Belew, R.K.;Goodsell, D.S.; Olson, A.J. AutoDock4 and AutoDockTools4: Automated docking with selective receptor flexibility. *J. Comput. Chem.* **2009**, *30*, 2785–2791. [[CrossRef](#)]

27. Seeliger, D.; de Groot, B.L. Ligand docking and binding site analysis with PyMOL and Autodock/Vina. *J. Comput. Aided. Mol. Des.* **2010**, *24*, 417–422. [[CrossRef](#)]
28. Laible, M.; Boonrod, K. Homemade site directed mutagenesis of whole plasmids. *J. Vis. Exp.* **2009**, *27*, e1135. [[CrossRef](#)]
29. Smith, P.K.; Krohn, R.I.; Hermanson, G.T.; Mallia, A.K.; Gartner, F.H.; Provenzano, M.D.; Fujimoto, E.K.; Goeke, N.M.; Olson, B.J.; Klenk, D.C. Measurement of protein using bicinchoninic acid. *Anal. Biochem.* **1985**, *150*, 76–85. [[CrossRef](#)]
30. Ying, X.; Yu, S.; Huang, M.; Wei, R.; Meng, S.; Cheng, F.; Yu, M.; Ying, M.; Zhao, M.; Wang, Z. Engineering the enantioselectivity of yeast old yellow enzyme OYE2y in asymmetric reduction of (*E/Z*)-citral to (*R*)-citronellal. *Molecules* **2019**, *24*, 1057. [[CrossRef](#)] [[PubMed](#)]